

# Heat capacity of the quantum magnet $\text{TiOCl}$

J. Hemberger<sup>1</sup>, M. Hohenknecht<sup>2</sup>, M. Klemm<sup>2</sup>, M. Sing<sup>2</sup>, R. Claessen<sup>2</sup>, S. Horn<sup>2</sup>, and A. Loidl<sup>1</sup>

<sup>1</sup>Experimentalphysik V, Center for Electronic Correlations and Magnetism,  
Universität Augsburg, D-86135 Augsburg, Germany

<sup>2</sup>Experimentalphysik II, Institut für Physik, Universität Augsburg, D-86135 Augsburg, Germany

Measurements of the heat capacity  $C(T;H)$  of the one-dimensional quantum magnet  $\text{TiOCl}$  are presented for temperatures  $2\text{ K} < T < 300\text{ K}$  and magnetic fields up to  $5\text{ T}$ . Distinct anomalies at  $91\text{ K}$  and  $67\text{ K}$  signal two subsequent phase transitions. The lower of these transitions clearly is of first order and seems to be related to the spin degrees of freedom. The transition at  $92\text{ K}$  probably involves the lattice and/or orbital moments. A detailed analysis of the data reveals that the entropy change  $S$  through both transitions is surprisingly small ( $< 0.1R$ ), pointing to the existence of strong fluctuations well into the non-ordered high-temperature phase. No significant magnetic field dependence was detected.

PACS numbers: 71.30.+h, 72.80.Ga, 65.40.Ba

## I. INTRODUCTION

The discovery of high- $T_c$  superconductivity in the cuprates and of colossal magnetoresistance in manganite perovskites generated an enormous interest in transition-metal oxides (TMOs). TMOs are characterized by an intimate coupling of spin, charge, orbital and lattice degrees of freedom which is the origin of a number of complex and exotic ground states. The discovery of a number of new low-dimensional spin  $1/2$  quantum magnets was another result of this renewed interest. After the first experimental observation of a spin-Peierls scenario in the organic compound  $\text{TTF-CuBDT}$ <sup>1</sup> more than 30 years ago,  $\text{CuGeO}_3$ <sup>2</sup> was the first inorganic spin-Peierls system. Another paradigmatic example is  $\text{NaV}_2\text{O}_5$ ,<sup>3</sup> a spin ladder with mixed-valent vanadium ions undergoing a charge ordering transition<sup>4</sup>. Further interest in these low-dimensional quantum magnets comes from the fact that upon doping they may undergo metal-to-insulator transitions and possibly reveal superconductivity. During the last decade  $\text{TiOCl}$  has been a distinguished candidate for a resonating-valence bond ground state<sup>5</sup> and has emerged as a further quantum spin magnet with a gapped ground state<sup>5,6</sup>.

Titanium-oxochloride has first been synthesized by Friedel and Guerin in 1876.<sup>7</sup> The first detailed report on growth and characterization has been given by Schäfer et al.<sup>8</sup> almost 50 years ago.  $\text{TiOCl}$  crystallizes in the orthorhombic  $\text{FeOCl}$  structure, consisting of  $\text{TiO}$  bilayers separated by  $\text{Cl}$  layers. In this structure every  $\text{Ti}$  is surrounded by 4 oxygen and 2 chlorine ions forming a distorted octahedron. Originally, based on an analysis of susceptibility data combined with band-structure calculations, it has been suggested that the  $t_{2g}$  orbitals are orbitally ordered, producing one-dimensional antiferromagnetic  $S = 1/2$  chains<sup>6</sup>. The high-temperature magnetic susceptibility could well be described by a Bonner-Fisher type of behavior with an exchange constant  $J = 660\text{ K}$ . A sudden drop of the susceptibility almost to zero indicated the opening of a spin gap at  $T_{c1} = 67\text{ K}$ , while a further anomaly has been detected at  $T_{c2} = 95\text{ K}$ . Electron spin

resonance<sup>9</sup>, infrared and Raman spectroscopy<sup>10,11</sup> as well as NMR measurements<sup>12</sup> substantiated these results and established a spin gap of the order of  $430\text{ K}$ . The origin of the gap has been identified as due to a first order spin-Peierls transition at  $T_{c1}$ , as evidenced by the observation of dimerization in temperature-dependent x-ray diffraction.<sup>13</sup> The nature of a second transition at  $T_{c2}$  is still unclear. While a broadening of the NMR lineshape into a wide continuum below  $T_{c2}$  has been attributed to a possible incommensurate (orbital) ordering<sup>12</sup>, no corresponding superlattice reflections could be observed in x-ray scattering,<sup>13</sup> though there is some evidence for a structural symmetry lowering from the high-temperature phase. Close to  $T = 135\text{ K}$  the opening of a spin pseudo gap as detected in NMR<sup>12</sup> and the onset of giant phonon anomalies in infrared and Raman spectroscopy<sup>11</sup> indicated the presence of strong spin fluctuations and a pronounced coupling to the lattice, respectively, for temperatures up to  $T = 135\text{ K}$ .

Electronically,  $\text{TiOCl}$  is a Mott insulator with nominally trivalent  $\text{Ti}$ . Electronic structure calculations using the LDA + U predict a  $\text{Ti} 3d_{xy}^1$  ground state,<sup>6,14</sup> however, coupling to optical phonon modes can lead to strong orbital fluctuations within the  $t_{2g}$  crystal field multiplet. The importance of correlation effects has been elucidated in LDA + DMFT<sup>15,16</sup> studies.

In this brief experimental report we provide detailed measurements of the heat capacity of  $\text{TiOCl}$  to further unravel the nature of the two phase transitions.

## II. EXPERIMENTAL DETAILS

Single crystals of  $\text{TiOCl}$  were prepared by chemical vapour transport from  $\text{TiCl}_3$  and  $\text{TiO}_2$ .<sup>8</sup> The samples have been characterized using x-ray diffraction, SQUID and ESR measurements at X-band frequencies. The crystal symmetry was found to be orthorhombic with lattice parameters of  $a = 0.379\text{ nm}$ ,  $b = 0.338\text{ nm}$  and  $c = 0.803\text{ nm}$ . The magnetic properties were found to be in excellent agreement with published results<sup>6,9</sup>. The

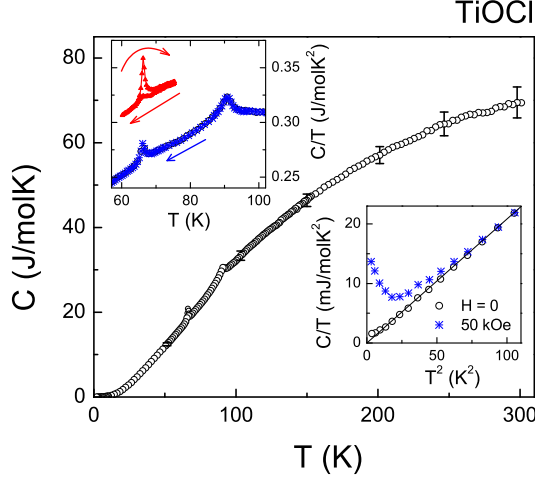


FIG. 1: Heat capacity of  $\text{TiOCl}$  vs. temperature. The vertical bars indicate experimental uncertainties and reveal the scatter of  $C(T)$  in different measuring cycles with different temperature stimuli and using different samples. Upper inset: Magnified region of the two phase transitions. The heat capacity measured at 5 T (stars) is compared to the heat capacity in zero external field (circles), both measured on cooling. The temperature region around the lower transition at  $T_{c1} = 66.7$  K was remeasured (triangles) utilizing a reduced relaxation amplitude of  $T = 0.5$  K on heating and subsequent cooling. For clarity these data are shifted by  $50 \text{ mJ/molK}^2$ . Lower inset: Low-temperature heat capacity plotted as  $C/T$  vs.  $T^2$ . For the results in zero magnetic field a fit using a Debye-derived phonon contribution is indicated as solid line.

heat capacity measurements have been performed with a commercial PPM S from Quantum Design for temperatures  $1.8 \text{ K} < T < 300 \text{ K}$  and in external magnetic fields up to 5 T.

### III. RESULTS AND DISCUSSION

Fig. 1 shows the central result of this investigation, the heat capacity as function of temperature. The heat capacity is characteristic for a three-dimensional solid with a Debye temperature of order 200 K. Superimposed we find two weak but distinct anomalies which are clearly related to the two subsequent phase transitions at  $T_{c1} = 67 \text{ K}$  and  $T_{c2} = 91 \text{ K}$ . In recent NMR experiments<sup>12</sup> slightly different temperatures, namely 94 K and 66 K, respectively, have been determined. The effects of the phase transitions on the specific heat are remarkably weak and are almost lost under the large phonon-derived heat-capacity contributions, and it is clear that the entropy covered by the two anomalies is comparably small.

The upper inset in Fig. 1 shows the heat capacity (given as  $C/T$  vs.  $T$ ) in the temperature region of the

phase transitions for both zero field and an external magnetic field of 5 T measured on cooling together with a special heating/cooling run in the vicinity of  $T_{c1}$  in zero-field, which will be discussed later.

Concerning the magnetic field dependence we observe no effects on the heat capacity within experimental uncertainties. The moderate magnetic fields used here neither shift the transition temperatures, nor do they seem to affect the entropies involved in the phase transitions. On the other hand, the small energy of our fields of order  $50 \text{ kOe} \approx 0.06 \text{ meV}$  is negligibly small compared to the intrinsic magnetic energy scale of  $\text{TiOCl}$  as estimated from  $k_B T_{c1/2}$  (5.8 and 7.9 meV) or the exchange constant  $J$  (57 meV).

In order to analyze the nature of the detected anomalies in terms of first or second order phase transitions, we performed heating/cooling cycles across the phase transitions. As the experimental setup utilizes a relaxation method, each data point is related to the average over a temperature interval above the initially stabilized temperature rather than to an exact temperature.<sup>17</sup> This means, that for the cooling sequence the temperature is decreased between the data acquisition and increased during the acquisition process itself. Thus, in the case of hysteretic (i.e. first order) behavior, the actual transition, together with the corresponding release of latent heat, only is fully captured only in the heating branch of the measuring sequence. A round  $T_{c1}$  a significant difference between heating and cooling can be detected, pointing towards a first order transition (shifted curve in the inset of Fig. 1). No such feature could be found for the upper transition at  $T_{c2}$ .

The lower inset in Fig. 1 shows the low-temperature heat capacity plotted as  $C/T$  vs.  $T^2$  to search for possible spin contributions. In zero external magnetic field,  $C(T)$  is fully determined by phonon contributions and from a linear fit (solid line) a Debye temperature of  $\theta_D = 210 \text{ K}$  can be determined. The low-temperature heat capacity becomes slightly enhanced in magnetic fields of 5 T which can be explained by the increasing importance of nuclear hyperfine contributions or the influence of paramagnetic defects at the lowest temperatures. For comparison, the low-temperature specific heat of the canonical organic spin-Peierls compound  $(\text{MTTF})_2\text{PF}_6$ <sup>18</sup> displays besides the nuclear hyperfine and  $T^3$  phonon contributions an additional quasi-linear ( $T^{1/2}$ ) term which has been ascribed to low-energy excitations. A similar contribution certainly can be excluded for  $\text{TiOCl}$ .

In the following analysis we will decompose the heat capacity into phonon and spin ( $S = 1/2$ ) contributions, with the former dominating the latter for all temperatures. Nevertheless, we are able to perform a straightforward analysis of the thermal properties of  $\text{TiOCl}$  and we will show that we arrive at a rather consistent description despite the large uncertainties mentioned above.

Fig. 2 shows the heat capacity for the complete temperature regime investigated, plotted as  $C/T$  vs.  $T$ . Assuming a  $S = 1/2$  spin chain the contribution of the spin

chain for  $T > 67$  K is modelled by a Bonner-Fisher type of behavior<sup>19</sup> taking into account an exchange coupling  $J = 660$  K. For the low-temperature regime, i.e. below the spin-Peierls transition at  $T_{c1} = 67$  K, the expected exponential decrease of the spin part of the heat capacity is simulated by a BCS-like mean-field treatment<sup>20</sup> with a temperature dependent gap,  $2\Delta_0 = 3.5k_B T_{c1}$ , and, at  $T_{c1}$ , a heat capacity jump of 1.43 times the contribution of the spin-chain, as it was proposed for canonical spin-Peierls systems.<sup>1</sup> Using this approach we can calculate the spin-derived heat capacity without any free parameter. The result (for representation multiplied by a factor of 3) is shown as dash-dotted line in Fig. 2. We are aware that this can only be a very rough analysis, specifically having in mind that the actual gap in  $\text{TiOCl}$  seems to be much larger and has recently been determined as  $2\Delta = 10 - 15k_B T_{c1;c2}$  by NMR experiments<sup>12</sup> and that the transition actually is of first order. The disregard of these experimental facts gives an underestimation of the jump height of the magnetic specific heat at the spin-Peierls transition and a too broad decay below, leading indeed to observable differences between the measured data and our calculation closely below  $T_{c1}$ . However, the overall entropy balance is not affected by these shortcomings of our simple model. The total magnetic entropy at high temperatures sums up to  $R \ln 2$  as expected for a spin 1/2 system.

The phonon system has been treated assuming one

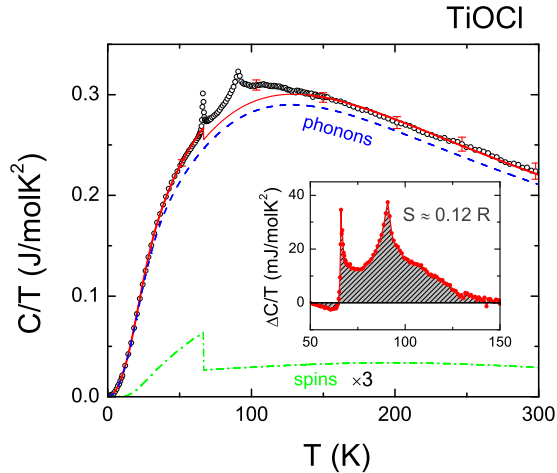


FIG. 2: Heat capacity of  $\text{TiOCl}$  plotted as  $C/T$  vs.  $T$ . The  $S = 1/2$  contribution including a mean-field spin-Peierls transition as described in the text is indicated as dash-dotted line. For representation purposes the calculated values have been multiplied by a factor of 3. The fit to the phonon-derived specific heat (see text) is indicated as dashed line. The sum of both contribution is drawn as solid line and represents the best fit to the experimental results. The inset shows the difference between calculated and measured heat capacities in a limited temperature regime.

Debye- and two Einstein-type contributions, yielding a total of 5 free parameters, namely, the mean Debye ( $\theta_D$ ) and two Einstein temperatures ( $\theta_{E1,2}$ ), and the ratio of Debye to Einstein modes  $R_{D=E}$ , as well as the ratio between the Einstein modes  $R_{E1=E2}$ . The number of degrees of freedom ( $N_f$ ), which of course should be nine per formula unit of  $\text{TiOCl}$ , was kept fixed. The experimentally determined heat-capacity values for  $2\text{ K} < T < 65\text{ K}$  and  $130\text{ K} < T < 300\text{ K}$  have been used for the fit of the heat capacity. For the fitting procedure we included the spin contributions which have been calculated parameter-free as outlined above. The total heat capacity, spin and phonon contributions are shown as solid line in Fig. 2. The lattice derived heat capacity is indicated as dashed line. Despite this oversimplified model we arrive at an astonishingly good description of the heat capacity over the complete temperature range. The parameters as determined by the best fit seem to be realistic: The characteristic temperatures,  $\theta_D = 188\text{ K}$ ,  $\theta_{E1} = 352\text{ K}$ , and  $\theta_{E2} = 614\text{ K}$ , with the ratios  $R_{D=E} = 0.30$  and  $R_{E1=E2} = 0.51$  determining the relative weight of Debye and Einstein modes, are reliable keeping in mind that the optical phonon modes in  $\text{TiOCl}$  range from approximately  $100\text{ K}$  to  $700\text{ K}$  with dominant modes close to our values for  $\theta_{E1,2}$ .<sup>10,11</sup> The small discrepancy of the Debye temperature obtained from this overall fit to  $C(T)$ , compared to the value derived from the low-temperature heat capacity only, can be explained by the presence of relatively low lying optical modes.

Comparing the model heat capacity to the measured one in Fig. 2 we find very good agreement for the smooth temperature evolution for low ( $T < T_{c1}$ ) and high ( $T > T_{c2}$ ) temperatures. As clearly seen, the main deviations arise in the temperature region between the two phase transitions. The good agreement concerning the smooth part of the heat capacity may seem surprising in the light of our simplified model. On the other hand, the phonon part of our  $C(T)$ -model is reasonably close to a realistic description involving the true phonon spectrum and the spin part of the heat capacity bears only a small weight. Thus, we believe that our model yields a reliable estimate of the regular part of the specific heat, allowing us to separate out the anomalous contribution due to the phase transitions at  $T_{c1}$  and  $T_{c2}$ . The inset of Fig. 2 shows this extra heat capacity in a limited temperature range from  $50$  to  $150\text{ K}$ . The integral over this region gives an estimate of the entropy  $S$  being released when going through both transitions.  $S$  is of the order of  $0.12 R$  ( $0.02 R$ ) vanishingly small compared to  $R \ln(2)$  expected for a spin  $S = 1/2$  system or an orbital doubly degenerate state. The narrow peak at  $T_{c1}$  corresponds to the latent heat released at the phase transition where according to magnetic measurements spin dimerisation appears. The larger fraction of the entropy is covered under the phase transition at  $T_{c2}$  extending up to  $135\text{ K}$ , exactly the temperature where in NMR experiments the opening of a pseudo gap has been detected<sup>12</sup>. Assuming that the phonon and spin derived heat capacities are

correctly described, we are left with the orbital degrees of freedom only. However, if the orbitals undergo an ordering transition at  $T_{c2}$  the entropy again is much too low and orbital fluctuations must extend to much higher temperatures, even far above  $T_c$ , the characteristic temperature of the opening of a pseudo gap. In this sense our results are compatible with the strong fluctuation effects observed in NMR<sup>12</sup> and in Raman scattering<sup>11</sup> and with the results of density-functional calculations suggesting that TiOCl may be subject to strong orbital fluctuations<sup>14</sup>. This indicates that the phase above  $T_{c1}$  is characterized by the presence of pronounced fluctuations retaining some sort of short range order and thereby delaying the release of the full entropy with temperature, as typical for one-dimensional systems. Unfortunately, our specific heat data do not allow us to decide on the precise microscopic nature of the fluctuations (spin-Peierls or orbital ordering).

#### IV. CONCLUSIONS

Summarizing, we have measured the heat capacity of TiOCl for temperatures  $2\text{ K} < T < 300\text{ K}$  and magnetic fields up to  $5\text{ T}$ . We observed two anomalies at  $T_{c1} = 91\text{ K}$  and  $T_{c2} = 67\text{ K}$  corresponding to two subsequent phase transitions. The phase transition at  $67\text{ K}$ , where strong

spin-dimerization sets in, reveals significant hysteresis effects and hence is of first order. Most probably the orbital degrees of freedom are involved in the phase transition at  $T_{c2}$ , which shows no thermal hysteresis. The entropy below this anomaly is vanishingly small indicating that the largest fraction of entropy is released at considerable higher temperatures. The total heat capacity can satisfactorily be explained describing the phonon spectrum with Debye and Einstein modes and the magnetic excitations by a Bonner-Fisher type heat capacity for  $T > T_{c1}$  and the opening of a spin gap below. At low temperatures and zero external fields the heat capacity can satisfactorily be described taking a phonon-derived  $T^3$  term into account only. No indication of contribution of low-energy excitations can be detected.

#### Acknowledgments

We want to thank R. Valenti, J. Deisenhofer, and H.-A. Kug von Nidda for helpful discussions. This work was partly supported by the Bundesministerium für Bildung und Forschung (BM BF) via Grant No. VD I/EKM 13N 6917-A and by the Deutsche Forschungsgemeinschaft (Sonderforschungsbereich 484 in Augsburg and project CL 124/3-3).

- 
- <sup>1</sup> J.W. Bray, H.R. Hart, Jr., L.V. Interrante, I.S. Jacobs, J.S. Kasper, G.D. Watkins, S.H. Wee, and J.C. Bonner, Phys. Rev. Lett. 35, 744 (1975)
  - <sup>2</sup> M. Haase, I. Terasaki, and K. Uchinokura, Phys. Rev. Lett. 70, 3651 (1993)
  - <sup>3</sup> M. Isobe, Y. Ueda, J. Phys. Soc. Jpn. 65, 1178 (1996)
  - <sup>4</sup> J. Ludecke, A. Jobst, S. van Smaalen, E. Morre, C. Geibel, H.-G. Krane, Phys. Rev. Lett. 82, 3633 (1999); M. Lohmann, H.-A. Kug von Nidda, M. V. Eremenko, A. Loidl, G. Oelmüller, S. Horn, Phys. Rev. Lett. 85, 1742 (2000)
  - <sup>5</sup> R. J. Beynon, J. A. Wilson, J. Phys. Condens. Matter 5, 1983 (1993)
  - <sup>6</sup> A. Seidel, C. A. Marianetti, F. C. Chou, G. Ceder, P. A. Lee, Phys. Rev. B 67, 020405(R) (2003)
  - <sup>7</sup> C. Friedel, J. Guerin, Ann. Chim. Physique 8, 36 (1876)
  - <sup>8</sup> H. Schafer, F. Wartenpfuhl, E. Waise, Z. anorg. und allg. Chemie 295, 268 (1958)
  - <sup>9</sup> V. Kataev, J. Baier, A. Möller, L. Jongen, G. Meyer, A. Freimuth, Phys. Rev. B 68, 140405 (2003)
  - <sup>10</sup> G. Caimi, L. Degiorgi, N. N. Kovaleva, P. Lemmens, F. C. Chou, Phys. Rev. B 69, 125108 (2004)
  - <sup>11</sup> P. Lemmens, K. Y. Choi, G. Caimi, L. Degiorgi, N. N. Kovaleva, A. Seidel, F. C. Chou, Phys. Rev. B 70, 134429 (2004)
  - <sup>12</sup> T. Imai and F. C. Chou, arXiv:cond-mat/0301425
  - <sup>13</sup> M. Shaz, S. van Smaalen, L. Palatinus, M. Hoinkis, M. Klemm, S. Horn, and R. Claessen, to be published
  - <sup>14</sup> T. Saha-Dasgupta, R. Valenti, H. Rosner, C. Gros, Europhys. Letters 67, 63 (2004)
  - <sup>15</sup> L. C. Cacci, M. S. Laad, E. Müller-Hartmann, arXiv:cond-mat/0410472 (2004)
  - <sup>16</sup> T. Saha-Dasgupta, A. Lichtenstein, R. Valenti, arXiv:cond-mat/0411631 (2004)
  - <sup>17</sup> J. C. Lashley, M. F. Hundley, A. Migliori, J. L. Sarrao, P. G. Pagliuso, T. W. Darling, M. Jaime, J. C. Cooley, W. L. Hults, L. Morales, D. J. Thoma, J. L. Smith, J. Boerio-Goates, B. F. Woodfield, G. R. Stewart, R. A. Fisher, N. E. Phillips, CRYOGENICS 43, 369 (2003)
  - <sup>18</sup> J. C. Lasjaunias, J. P. Brison, P. Monceau, D. Staresinic, K. Biljakovic, C. Carcel, J. M. Fabre, J. Phys. Condens. Matter 14, 837 (2002)
  - <sup>19</sup> J. C. Bonner, M. E. Fisher, Phys. Rev. 135, A 640 (1964)
  - <sup>20</sup> B. M. Uhlischlegel, Z. Phys. 155, 313 (1959)